POLITECNICO DI TORINO
Repository ISTITUZIONALE

Displacement and strain data-driven damage detection in multi-component and heterogeneous composite structures

(Article begins on next page)

22 December 2024

Displacement and strain data-driven damage detection in multi-component and heterogeneous composite structures

A. Pagani[*], M. Enea[†]

*Mul*² Lab, Department of Mechanical and Aerospace Engineering,
Politecnico di Torino, Corso Duca degli Abruzzi 24, 10129 Torino, Italy.

Abstract: This work introduces the use of Convolutional Neural Network (CNN) in combination with advanced structural theories for the damage detection of multi-component and composite structures. Well established Component-Wise (CW) models based on the Carrera Unified Formulation (CUF) are developed first to demonstrate the effect of localized damages on the mechanical performance of thin-walled beams and laminates. Finite element Monte Carlo simulations of randomly damaged structures are then used to generate a large database of full-field displacement and strain images. These images are lately feed into a dedicated CNN for training purpose and for the prediction of location and intensity of structural damages occurring in unseen scenarios. The results demonstrate the validity of the present approach and suggest the importance of adopting opportune structural models to carry out localized damage detection by image-driven AI. Overall, the research provides good confidence for future investigation and experimental testing.

Keywords: Damage detection, Convolutional Neural Network, Composites, Finite Element Analysis.

1   Introduction

Composite materials are widely used in the aeronautical industry, due to their excellent specific mechanical properties. Nevertheless, they may be subjected to severe degradation, for example due to ageing phenomena or operational loads. Moreover, damage and failure propagation are difficult to predict because of the intrinsic heterogeneity of these materials. Indeed, aircraft companies continue to follow a scheduled maintenance program in order to ensure that a failure does not compromise the operations success and safety. These programs are based on Non-Destructive Tests (NDT) such as visual inspection, eddy current, thermography and ultrasonic inspection [1]. However, NDTs have some shortcomings, such as i) difficulties in detecting damage in particular regions of the investigated structure, ii) the need to know a priori the possible location of damage and iii) a relevant demand in terms of operational

---

[*]Associate Professor. Corresponding author. E-mail: alfonso.pagani@polito.it
[†]PhD candidate. E-mail: marco.enea@polito.it

costs. For these reasons, in recent years structural health monitoring techniques (SHM) are becoming a key research topic.

The objective of SHM is the detection, localization, quantification and classification of damage [2]. Several techniques are being developed for SHM purposes in composite materials, such as Lamb-waves characterization [3, 4], the use of distributed optical fibre sensors (DOFS) [5, 6], and intelligent coating monitoring [7]. However, in recent years researchers are focusing their efforts in finding a way to retrieve the unknown relation that could exist between a measured quantity and the damage distribution. This relationship can be found, among the others, by adopting artificial intelligence (AI) techniques, such as Artificial Neural Networks (ANN).

Different type of input can be used to feed the neural network and make the latter learn the relationship between input and damage patterns. Some examples of adopted input are dynamic [8, 9] and static [10] parameters, frequency response functions (FRFs) [11], and wavelet transform coefficients [12]. Nevertheless, when dealing with more complex problems, ANNs could encounter some difficulties in terms of overfitting and bad generalization. Hence, a deep-learning technique called Convolutional Neural Network (CNN) [13] has recently been adopted for damage detection purposes through image recognition. In [14], convolutional neural networks and 2D wavelet transform are integrated for detection of damage location in rectangular laminated composite plates. A similar approach has been proposed in [15]. In this work, Lamb waves and CNNs are combined in order to detect and quantify ply delamination damage in composites. In [16], the authors propose a method where CNNs are used for modal parameters extractions. A classification algorithm is then built for multiple-damage cases. In [17], the authors combined CNN with two-dimensional Digital Image Correlation (DIC) for automated monitoring of surface cracks progression.

Several research works adopt static parameters images (strain or displacement) to find the unknown correlation with damage distribution in combination with CNN. In [18], a CNN is trained with numerically-simulated raw strain measurements for both detection and localization tasks on structural connections. In [19], a DIC [20] based monitoring technique is proposed. Two-dimensional axial strain images obtained from numerical analysis are used for CNN training. A damage identification method based on strain mode differences and inverse Finite Element Method (iFEM) is proposed in [21]. The main advantage of this approach is that strain mode differences only need a series of low order damaged data.

In the literature, raw data for CNN training are obtained trough classical FE models (as in [22]). These models are not able to detect some mechanical behaviour, such as shear or thickness stretching. These simplifications may lead to a misleading description of the effects due to localized damages (see for example delamination in composite material structures). In this context, the present paper wants to demonstrate the importance of structural modelling in the training of CNN. Thus, AI is coupled with high-order theory of structures hereinafter by using the Carrera Unified Formulation (CUF) [23].

In recent years, CUF has proven to provide very accurate 3D-like solutions with a very low computational demand in several fields, such as structural dynamics [24, 25], progressive failure analysis [26, 27], and variable angle tow composite mechanics [28], among others. The aforementioned capabilities of CUF are exploited in this research to create a more extensive simulation-based database for CNN training. In fact, by adopting a non-local hierarchical expansion of the generalized displacements, a Component-Wise (CW) formulation [29] can be implemented in the CUF framework. The advantages represented by the CW formulation for damage detection purposes are: i) the opportunity to accurately describe multi-component structures, since each component can be modelled with its own geometrical and mechanical features; ii) the possibility of introducing damages with independent anisotropy and intensi-

ties in each component of the structure.

The CW approach has already been employed in applications related to structural damage. More specifically, in [30], the effect of localized damage on the vibrational characteristics of aircraft structures has been investigated. On the other hand, in [9], the inverse problem was solved: damage intensities and location were predicted by feeding a neural network with the dynamic parameters of randomly damaged metallic thin-walled structures. This approach was then applied to composite laminates [31]; here, the results obtained were not as promising as those of previous studies on thin-walled structures. This was mainly due to the monolithical nature of laminates, leading to the necessity of higher-frequencies mode computation to obtain sufficient information for damage detection. For this reason, in the present research, the previously enlisted CUF capabilities are exploited for the training of convolutional neural network with displacement and/or strain field images extracted from static analysis of damaged composite laminates. The output of this CNN will be damage location and severity in each component of the structure.

The present paper is organized as follows: first, CUF models are introduced, with a focus on the CW approach and the damage modelling; subsequently, the working principles of the CNN are presented. Then, the numerical results are shown and discussed. Finally, the main conclusions are drawn.

2 Component-wise models

Simulation-based damage detection required effective and efficient models able to describe localized phenomena and three-dimensional effects. High-order structural theories might be adopted to satisfy this necessity. As a matter of fact, a sufficiently enriched displacement kinematics can provide the same accuracy of 3D solutions with significantly low computational costs. In the present work, the Carrera Unified Formulation (CUF) is employed to automatically develop refined finite elements with scalable accuracy. The main capabilities of CUF are introduced in this section.

2.1 Carrera Unified Formulation

One-dimensional (1D), two-dimensional (2D) structural models and any combinations of thereof can be developed in the framework of CUF. For simplicity, let us first consider a generic beam with the main axis aligned along the y direction (Fig. 1a). The cross-section Ω is normal to the beam axis y. The validity of the formulation is not affected by the shape of the cross-section although. The three-dimensional displacement field can be written as:

$$\mathbf{u}(x, y, z) = F_\tau(x, z)\mathbf{u}_\tau(y), \qquad \tau = 1, 2, ..., M \qquad (1)$$

where $\mathbf{u}(x, y, z)$ is the displacement vector; F_τ are generic functions over the cross-section coordinates x and z; $\mathbf{u}_\tau$ is the generalized displacement vector; M refers to the number of terms in the expansion; and the repeated subscript τ indicates summation.

2D models can be formulated similarly. With reference to Fig. 1b, the displacement kinematics of a plate element can be expresses as follows:

$$\mathbf{u}(x, y, z) = F_\tau(z)\mathbf{u}_\tau(x, y), \qquad \tau = 1, 2, ..., M \qquad (2)$$

where now F_τ is expressed along the thickness direction and the generalized displacements $\mathbf{u}_\tau$ are functions of the mid-plane coordinates.
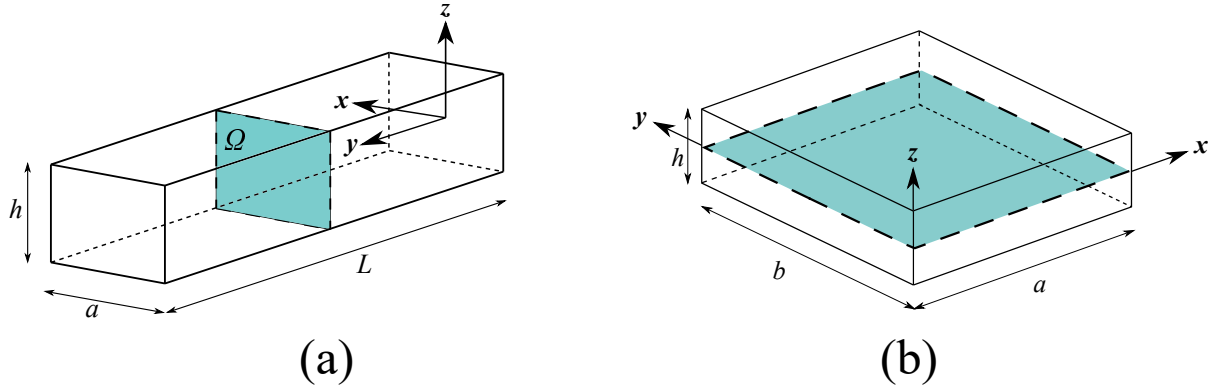
Figure 1: Geometry and reference system for a generic (a) beam and (b) plate.

It should be underlined that, for both beam and plate models, the functions adopted to model the displacement field across the section (1D) or through the thickness (2D) can be arbitrary and tuned depending on the characteristics of the structural problem considered. As an example, one may recall that classical structural theories generally utilized in practical engineering problems (e.g., Timoshenko beam theory or Reissner-Mindlin plate theory) make use of a combination of constant and linear F_τ functions. These classical theories are particular (degenerated) cases of what in terms of CUF formalism are known to as Taylor Expansion (TE) models. TE models, in detail, employ Mclaurin polynomials of truncated order N to develop hierarchical low- to high-order kinematics. TE CUF-based model have been extensively used in previous research with good results. However, these models could give some inaccuracies when dealing with some particular problems, such as complex thin-walled beams or thick composite plates. For more demanding structural simulations, indeed, LE (Lagrange Expansion) CUF-based finite elements were developed by Petrolo and Carrera [32].

LE models use a combination of Lagrange polynomials as expanding functions F_τ. Their main feature is that they have only pure displacement variables and can be used to provide a non-local expansion of the theory kinematics over structural sub-domains. This is one of the essential characteristics of the CW approach, which is described in the next section.

2.2 Finite element approximation

The finite element method is adopted in this work to discretize the generalized unknowns within the support (either 1D or 2D). In the case of beam structures, for example, $\mathbf{u}_\tau$ can be approximated by using 1D classical shape functions N_i to have:

$$\mathbf{u}(x,y,z) = F_\tau(x,z)N_i(y)\mathbf{q}_{\tau i}, \qquad \tau = 1,...,M, \ i = 1,...,p+1 \tag{3}$$

where N_i stands for the shape functions of order p and $\mathbf{q}_{\tau i}$ is the nodal displacement vector. Plate finite elements can be formulated similarly. The shape functions are not given here, but they are presented in several works, for example in [33]. In the case of beam models, elements with cubic approximation have been adopted in this work. The cross-section discretization for the LE class is entirely independent of the beam finite element's choice to be used along the axis of the beam.

The governing FE equations can be obtained via principle of virtual displacements, which reads:
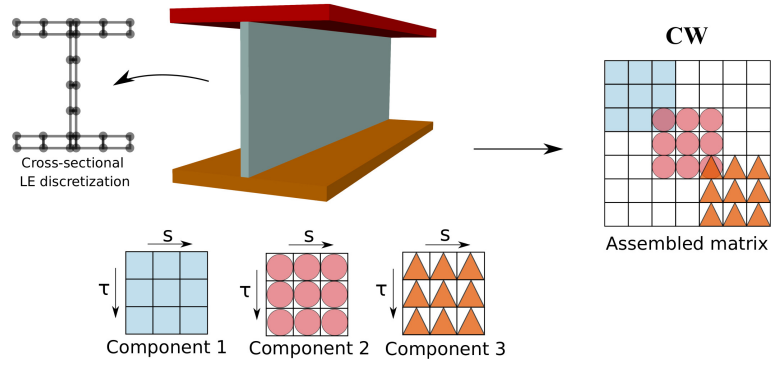
$$\delta L_{\text{int}} = \delta L_{\text{ext}} \tag{4}$$

4

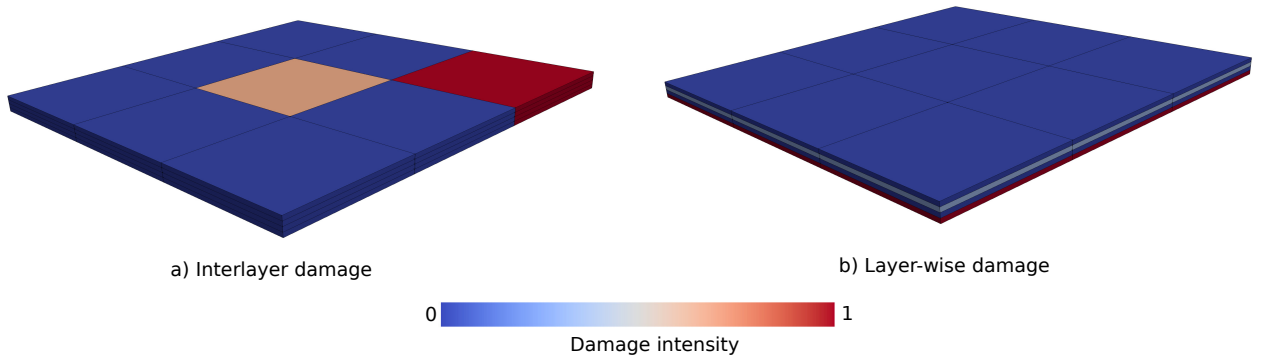Figure 2: Global matrix assembly in a component-wise approach. Each colour represents a different component.

a) Interlayer damage

b) Layer-wise damage

Damage intensity

Figure 3: Examples of component-wise damage modelling.

where δL_{int} and δL_{ext} are the virtual variation of strain energy and work of external loadings, respectively. Substituting Eq. (3), considering the generalized Hooke law, the linear geometrical relations and after some manipulations, the governing equation will read as:

$$\mathbf{K}^{ij\tau s}\mathbf{q}_{\tau i} - \mathbf{p}_{sj} = 0 \qquad (5)$$

where $\mathbf{K}^{ij\tau s}$ and and $\mathbf{p}_{sj}$ are the fundamental nuclei of the the stiffness matrix and the nodal loading vector, respectively. $\mathbf{K}^{ij\tau s}$ is a 3x3 matrix that can be expanded by looping over the indexes τ, $s = 1, 2, .., M$ and i, $j = 1, 2, ..., p+1$ to obtain the stiffness matrix of arbitrarily enriched finite elements. After assemblying over the finite element discretization, the final system of algebraic equations is obtained:

$$\mathbf{K}\mathbf{q} - \mathbf{p} = 0 \qquad (6)$$

where $\mathbf{K}$, $\mathbf{q}$ and $\mathbf{p}$ are the assembled arrays of the final structure.

3 Component-wise damage formulation

Figure 2 shows a CW modelling approach for an I-section beam with three components, two flanges and the web. Each component can be modelled with one or more LE beam element. Then, each LE element is assembled above the cross-section to obtain the global stiffness matrix, see [34]. Thanks to LE, indeed, displacement compatibility at the component interface

5

can be guaranteed straightforwardly. One of the advantages of the CW formulation is the possibility of tuning the model capabilities by i) choosing a specific degree of accuracy for each component and ii) setting the order of the structural model to be adopted. Furthermore, this approach allows the introduction of different damage intensities for each component, allowing a more localized damage distribution in the structure, if necessary.

In this research, both isotropic and orthotropic damage models have been implemented. In any case, for simplicity reasons, damage is simulated as stiffness reduction of the interested region. An example is shown in Fig. 3 for the case of a composite laminated plate. Here, there are two possible ways of introducing damage in the investigated structure. The first one provides a stiffness reduction through all the thickness of a composite section region, which in this example is divided into nine sampling areas. A second possibility is a layer-wise damage modelling: each layer will see a different damage intensity. Clearly, the two approaches can also be combined.

In the case of the isotropic damage, the Young moduli along all three directions are degraded by the same damage parameter d:

$$E_{ii}^d = (1 - d) \times E_{ii}, \text{ with } 0 \leq d \leq 1 \tag{7}$$

where E_{ii}^d and E_{ii} are the Young moduli in the three directions for the damaged and pristine structure, respectively, and d is the damage coefficient. This parameter can vary from a value of $d = 0$ to $d = 1$, representing a pristine and a completely failed component. However, this type of approach could represent a too strong simplification for the case of composite laminates, where properties can be significantly different between longitudinal and transversal directions. For this reason, an orthotropic damage modelling has been implemented too. Two parameters d_1 and d_2 are employed for the degradation of stiffness in each region in this case. They are used to modify the correspondent material matrix $\mathbf{C}$ as follows [35]:

$$\mathbf{C} = \frac{1}{\Delta} \begin{bmatrix} (1 - R_2\nu_{23}\nu_{32})R_1 E_{11} & (\nu_{21} + \nu_{23}\nu_{31})R_1 R_2 E_{11} & (\nu_{31} + R_2\nu_{21}\nu{32})R_1 E_{11} & 0 & 0 & 0 \\ & (1 - R_1\nu_{31}\nu_{13})R_2 E_{22} & (\nu_{32} + R_1\nu_{31}\nu{12})R_2 E_{22} & 0 & 0 & 0 \\ & & (1 - R_1 R_2\nu_{21}\nu_{12})E_{33} & 0 & 0 & 0 \\ & & & \Delta R_1 R_2 G_{12} & 0 & 0 \\ & & & & \Delta G_{23} & 0 \\ & sym & & & & \Delta G_{13} \end{bmatrix} \tag{8}$$

where $R_i = (1 - d_i)$, $i = 1, 2$ are the reduction factors and $\Delta = 1 - R_2\nu_{23}\nu_{32} - R_1 R_2\nu_{12}\nu_{21} - 2R_1 R_2\nu_{31}\nu_{12}\nu_{23} - R_1\nu_{31}\nu_{13}$. Thus, the parameter d_1 will reproduce a damage in the longitudinal direction, while the parameter d_2 indicates a damage in the transversal one, where both directions are referred to the material reference system.

4   CNN for damage detection

4.1   Architecture

A convolutional neural network is a specific deep learning architecture [36]. The main features of CNNs make this technique very suitable for image processing purpose. The main advantages of CNNs, compared to classical neural network, is the possibility of dealing with high dimensional input and with potentially overfitting algorithms. These objectives are addressed thanks to the local connectivity of a CNN: correlation between contiguous points is assumed.

This assumption ensures that each hidden unit is linked to just one subset provided from the previous layer. This method aims to reduce the number of learnable parameters involved and, by consequence, the computational demand of the CNN training. Another fundamental feature that makes CNNs suitable for image processing is their robustness to translation and distortion of the input [13].

Convolutional neural networks are fed with three-dimensional input. The network architecture which can receive and process these input can be built by employing three types of layers. Convolutional layers have two-dimensional learnable filters as parameters, which are made slide over the input layer. This layer computes the dot product between these filters and the current small region of the input, creating a feature map. These maps will be used as input for the following layers. Then, the pooling layer performs a downsampling operation using maximum or average operations. Finally, the fully-connected layer will compute the weighted sum of input as in classical feedforward neural network. It should also be underlined that regularization procedures are generally adopted in CNN training in order to prevent a bad generalization of the model to the non-training data. In the present work, dropout regularization and batch normalization layers are employed. An example of CNN architecture is shown in Fig. 4.
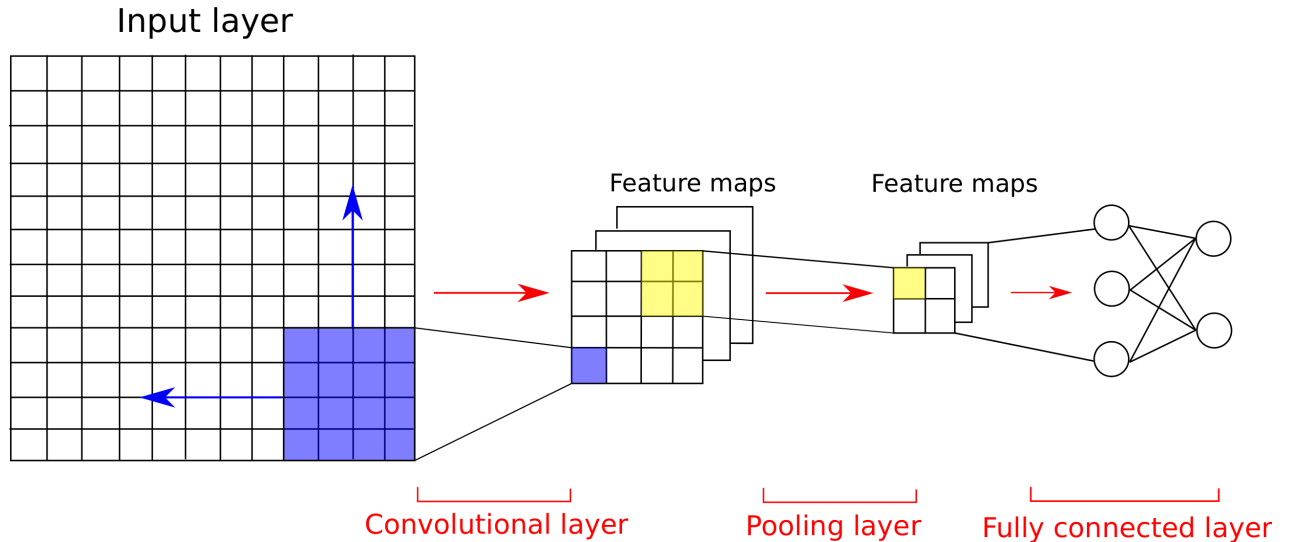

Figure 4: Example of CNN architecture.

4.2 Simulation-driven training process

A vast training database is needed for quantification and localization of damages in a structure. In order to build this database, the capabilities of CUF and the component-wise formulation are necessary for performing a large number of analysis with great accuracy, while reducing the required computational effort. Moreover, the CW approach gives the opportunity to provide a component-oriented localization of damage. In this work, the database has been created through CUF-based Monte Carlo simulations. Damage intensity has been assigned randomly to each component, following a Gaussian distribution, with mean and standard deviation equal to 0.1. Hence, a database of N samples has been built, aiming to cover the largest possible number of damage distributions. An example of database for the case of orthotropic damage modelling is shown in Table 1.

After damage maps are created, a component-wise simulation of each damaged structure is

	Component 1		Component 2		Component 3	
	d_1	d_2	d_1	d_2	d_1	d_2
Sample 1	0.11	0.20	0.02	0.01	0.16	0.23
Sample 2	0.23	0.05	0.24	0.06	0.00	0.14
Sample 3	0.02	0.15	0.034	0.06	0.15	0.12
...		...		...	...	...
...		...		...	...	...
Sample N	0.11	0.05	0.11	0.14	0.08	0.02

Table 1: Example of database of N samples for the three-component structure shown in Fig. 2. The damage introduced for each component is indicated in terms of longitudinal (d_1) and transversal (d_2) stiffness reduction.

carried out. The training process will be performed by feeding the CNN with representative displacement and/or strain field images. Finally, the CNN accuracy in predicting damage location and intensity is tested by employing images of potentially damaged and unseen structures. In Fig. 5, a flowchart representing the entire process is shown.
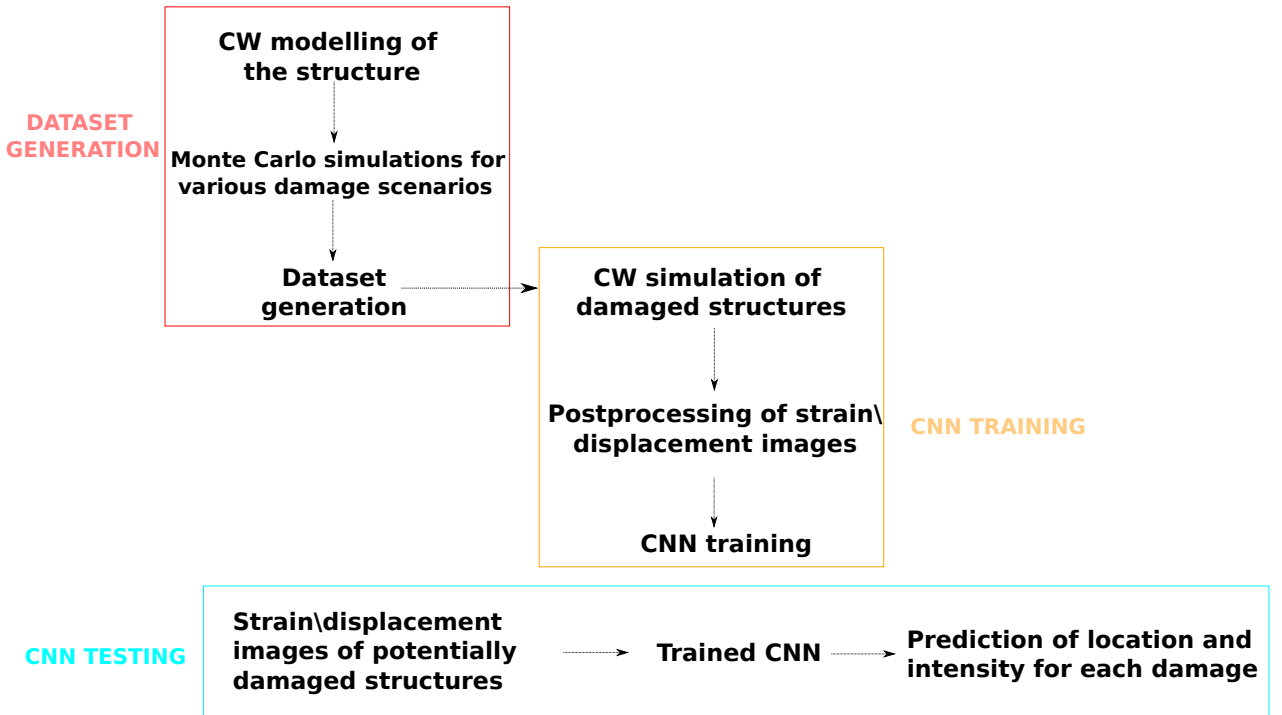

Figure 5: Flowchart representing the entire process for damage detection.

5 Numerical results

5.1 Effect of damage

In this section, the effect of damage localization and intensity on the structural behaviour of a thin-walled isotropic beam and a composite laminate is investigated. The following examples will point out the reason behind the necessity of adopting highest-fidelity and component-wise models for damage detection purposes.

5.1.1 Beam under bending and torsion

A cantilever I-section beam is considered as a first numerical case study. The beam is made of an isotropic material, with Young Modulus $E = 200$ GPa and Poisson ratio $\nu = 0.2$. The geometrical features and boundary conditions are shown in Fig. 6. First, a model assessment
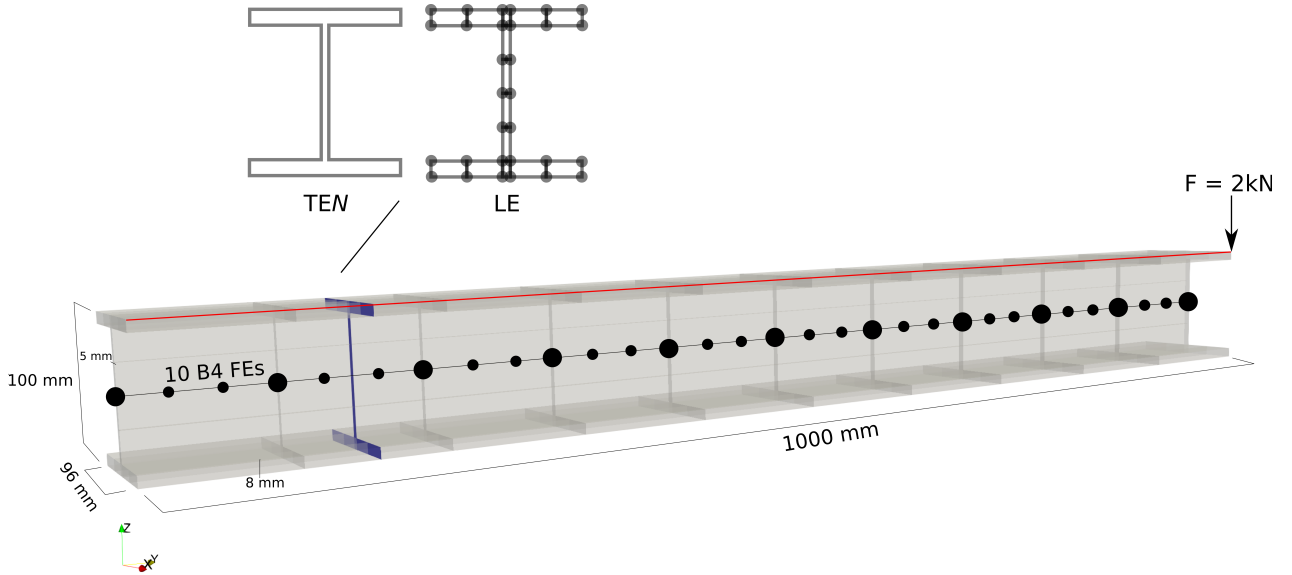

Figure 6: Geometrical and modelling features of an I-section beam subjected to point load.

is carried out. The reference solution is obtained through a commercial FE software, using 3D brick elements. Here, TE models (from linear TE1 to TEN refined) beam models as well as a CW piece-wise quadratic (referred to as LE9) beam models are employed and compared with the reference solution. In particular, the vertical displacement along the red line in Fig. 6 is considered. The outcome is displayed in Fig. 7. These results show how high accuracy can
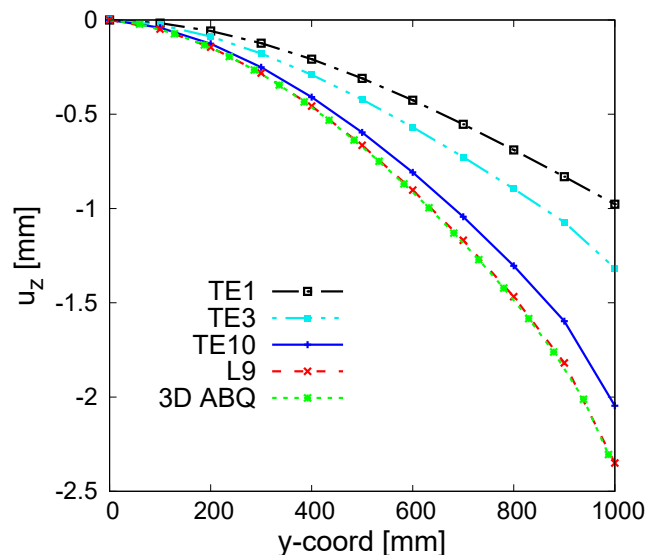

Figure 7: Comparison of the vertical displacement along the red line in Fig.6 adopting different theories. A numerical reference is provided by 3D Abaqus model.

be reached only if sufficiently rich kinematics is adopted for the CUF-based finite elements. In fact, the curve provided by the low-order TE1 model sees a significant discrepancy with

9

the Abaqus 3D simulation. However, a refinement of the employed theory leads to a closer solution, which is matched when high-order LE9 models are used.

A second numerical investigation on the I-section beam is now performed, in order to demonstrate the need of a component-wise approach for damage detection. Two different portions of the cross-section have been damaged. The extension of these areas is the same in both cases, as well as the intensity of the damage, which is equal to $d = 0.3$. These regions are placed in the right and left side of the upper cap, respectively (see red regions in Fig. 8). The damaged sections are introduced only near the clamped section, for $0 < y < 300$ mm, where a reduction in terms of stiffness is expected to have a bigger effect on the beam behaviour.
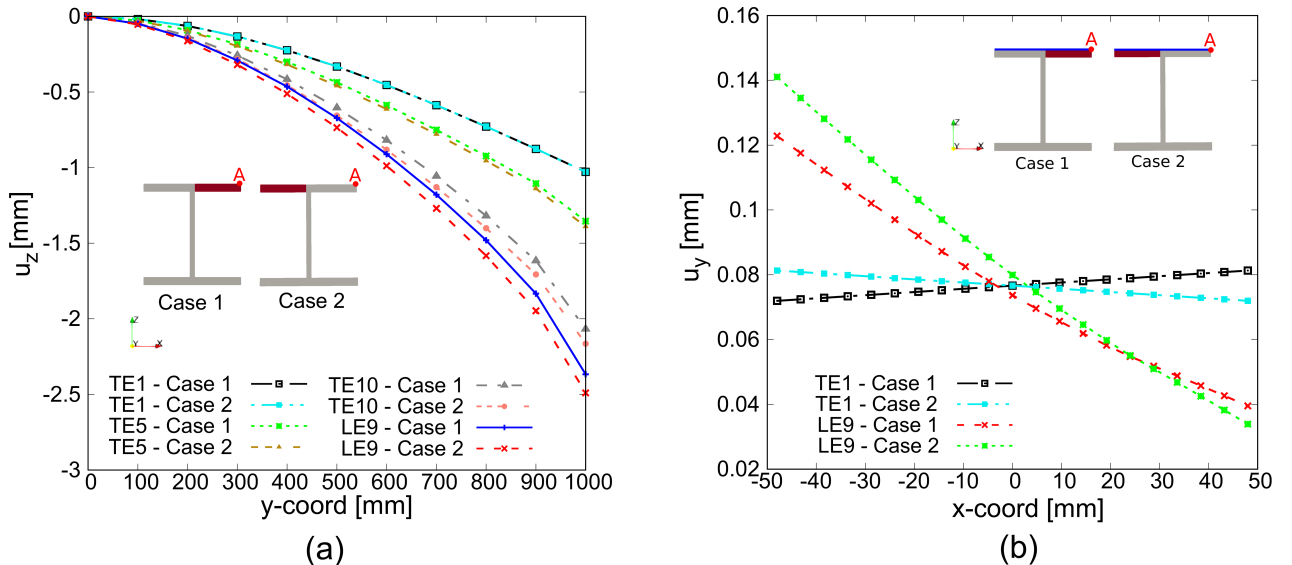

Figure 8: Comparison of a) vertical displacement along the red line in Fig. 6 and b) longitudinal displacement along the blue line at $y = 1000$ mm, adopting various theories and with two different damage cases. Point A represents the loading point.

Figure 8a shows the vertical component of the displacement along the red line for different FE models and for both damage cases. A first important indication is given by comparing the curves obtained adopting low-order TE1 models. In fact, this theory (comparable to classical beam models) can not detect any difference between the two damage cases, in terms of vertical displacement. This aspect represent a major shortcoming, especially when dealing with damage detection. However, Fig. 8a also shows that an enrichment of the beam kinematics can provide a better distinction between the two damage cases. Similar considerations are valid for the longitudinal displacement, evaluated along the blue line in Fig. 8b at the free section ($y = 1000$ mm). An almost constant value of u_y is retrieved when TE1 models are used, due to the beam rigid motion in the cross-section plane. However, in this case a difference between the two damage scenarios is found even with this low-order theory. On the other hand, using high-order LE theories leads to an accurate description of the warping phenomenon to which the structure is subjected.

5.1.2 Composite laminate under uniaxial traction

The second case study is a four-layer composite laminate, with stacking sequence $[90/0]_s$ (Fig. 9). The plies are of equal thickness and they are made of an orthotropic material, whose properties are enlisted in Table 2. The plate has one clamped edge, while the surface on

the opposite edge is subjected to uniaxial traction. The adopted mesh consists of three four-node cubic (B4) elements for the FEM discretization along the longitudinal axis, while three LE9 elements for each layer have been employed for the through-the-thickness discretization. Different damage scenarios have been implemented by considering nine distinct subportions of the whole domain. Each dagamed area involves the entire stacking trough the thickness (see interlayer damage in Fig. 3a).

E_{11} [MPa]	E_{22} [MPa]	E_{33} [MPa]	ν_{12}	ν_{13}	ν_{23}	G_{12} [MPa]	G_{13} [MPa]	G_{23} [MPa]
165.0	9.0	9.0	0.34	0.34	0.5	5.6	5.6	2.8

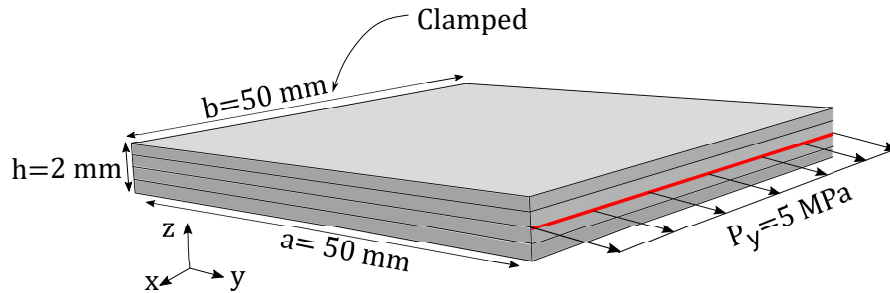Table 2: Material properties.

Figure 9: 3D model of the investigated composite laminate.

As a first analysis, the effect of damage location and intensity on the longitudinal displacement u_y along the middle surface of the laminate on one edge (red line in Fig. 9) is investigated. In Fig. 10, an isotropic interlaminar damage is introduced in a single region, with an intensity from 0, which refers to an pristine structure, to 0.5, which leads to a 50 % reduction of the region's stiffness. The isotropic damage modelling will be adopted for all analysis in the present section. It is easy to notice that damage location has a relevant effect on the maximum location of u_y. In fact, the maximum displacement will be in correspondence of the damaged region, due to the reduction of stiffness caused by the damage.
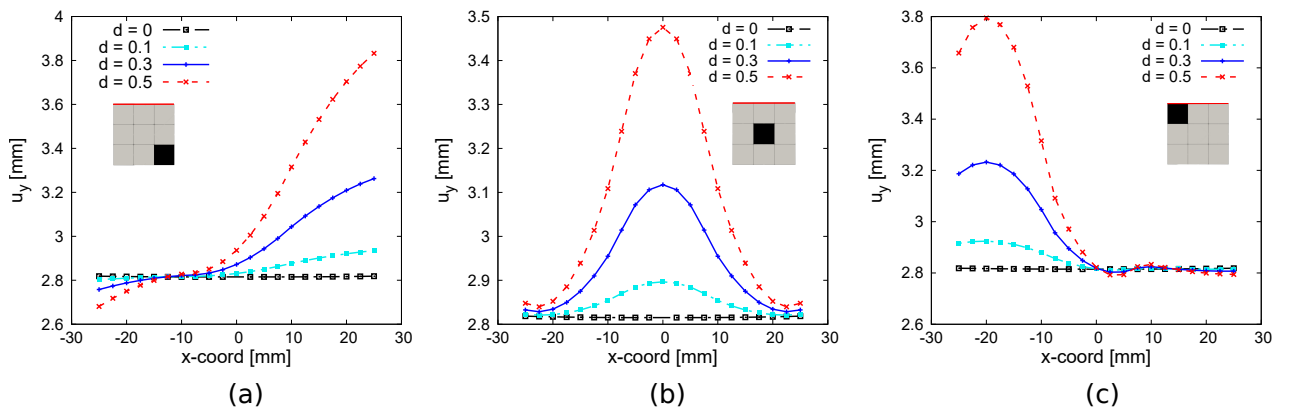

Figure 10: Effect of a single damaged region on longitudinal displacement u_y.

In Fig. 11, a group of three components is damaged at the same time. As in the previous case, the same damage is applied to all the four layers through the thickness. The damaged regions have a strong influence not only on the value of the maximum displacement, but also on the maximum location. To investigate the effect of layer-wise damage, instead, Fig. 12
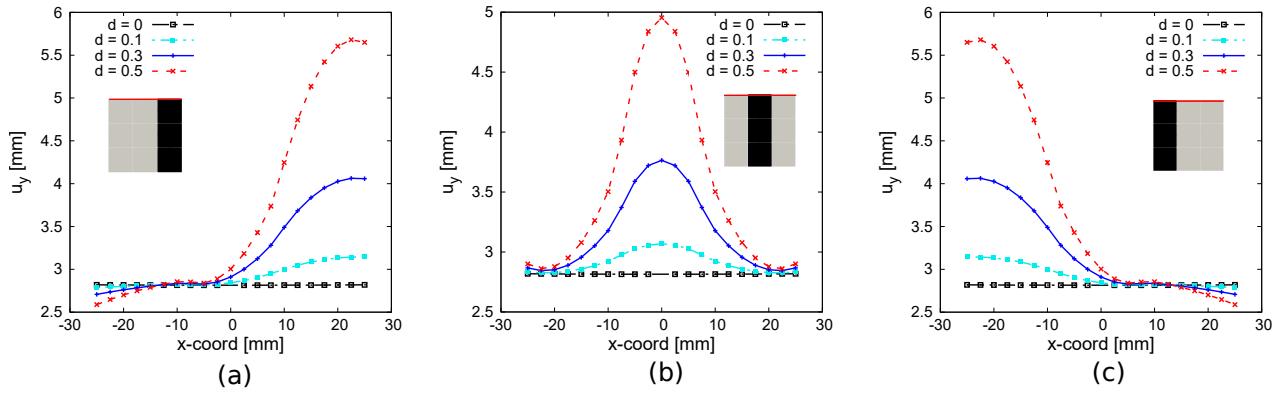
11

Figure 11: Effect of three damaged regions on longitudinal displacement u_y.
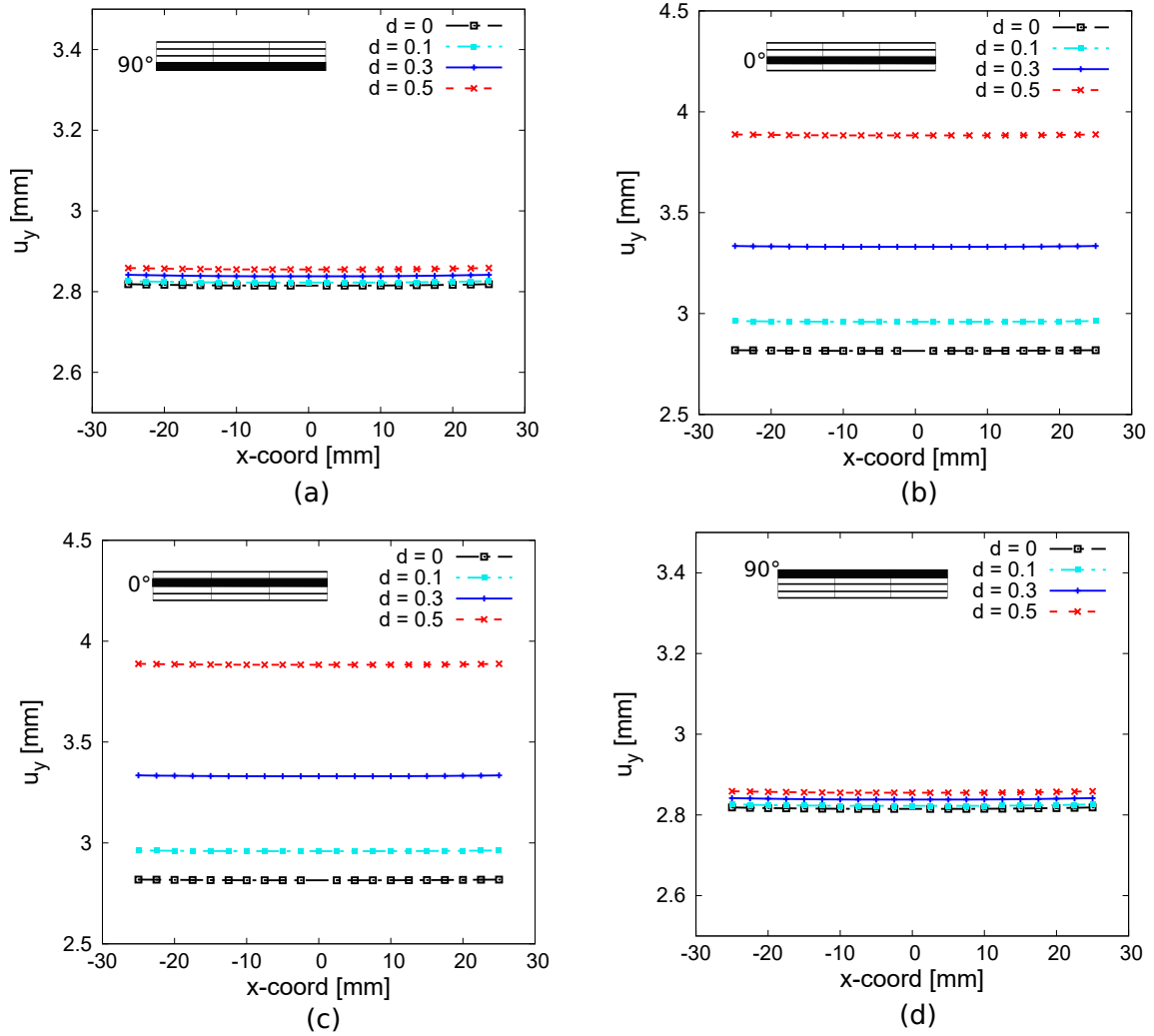

Figure 12: Effect of layer-wise damage modelling on longitudinal displacement u_y, evaluated along the red line.

shows the longitudinal displacement behaviour when a single layer is damaged. Furthermore, the influence of the stacking sequence on the u_y displacement is also studied. Four different laminations have been investigated. Namely:

- Lamination 1 : [45/0/0/45] - Symmetric

- Lamination 2 : [45/0/45/0] - Asymmetric

- Lamination 3 : [90/0/0/90] - Symmetric

- Lamination 4 : [90/0/90/0] - Asymmetric

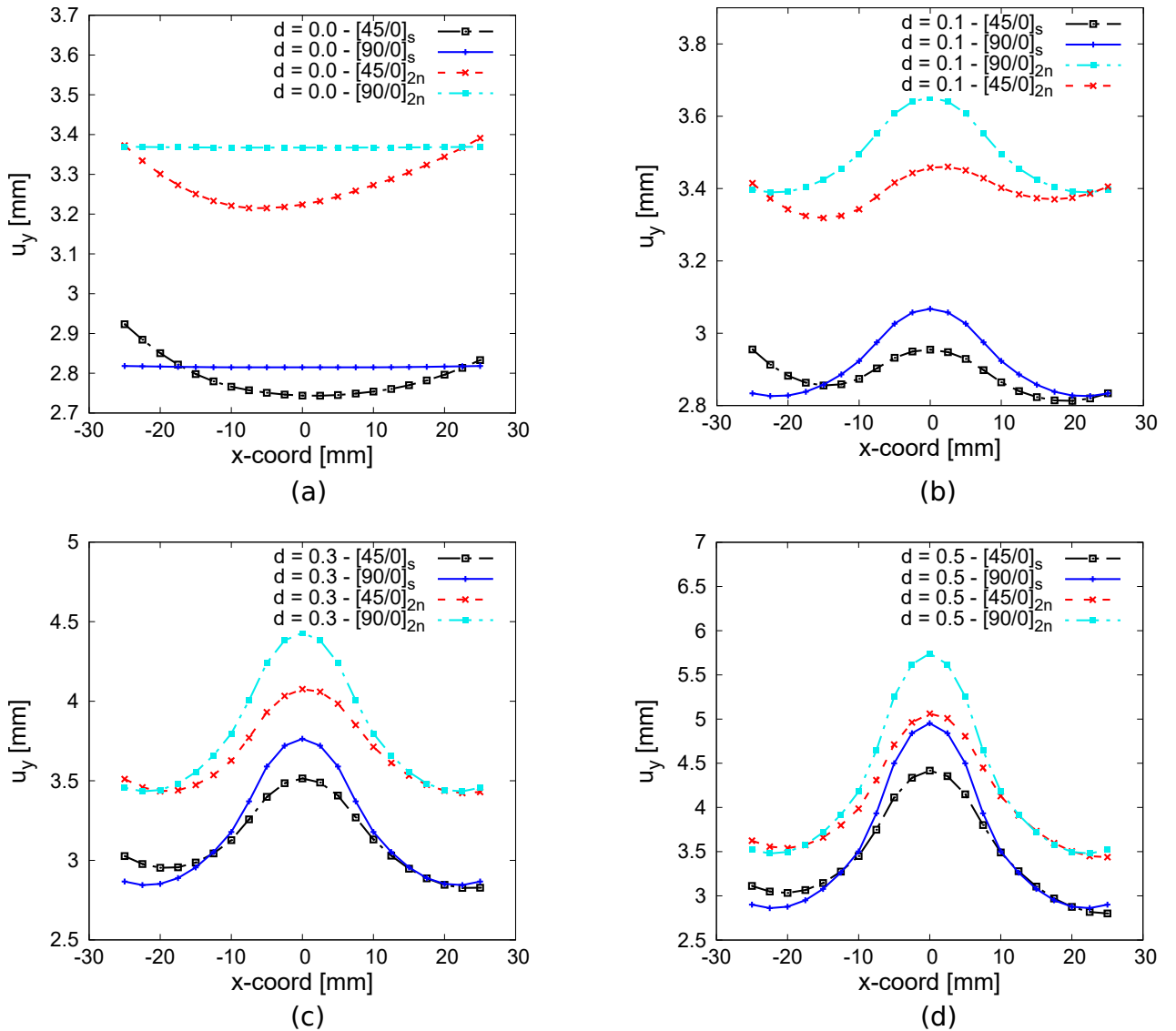The results for four different damage scenarios have been displayed in Fig. 13.

Figure 13: Effect of the stacking sequence on longitudinal displacement u_y at fixed level of damage.

5.1.3 Remarks about direct problem and damage simulation

The preliminary studies shown in Section 5.1 allow to make some practical considerations for CNN training and testing. In section 5.1.1, the importance of high-order theories and component-wise approach for damage detection has been demonstrated. In fact, low-order theories can not accurately describe some complex mechanical behaviours, such as bending and torsion in this case. This simplification leads to an incorrect description of the effects due to localized damages, making impossible their accurate detection by the CNN.

In section 5.1.2, the influence of damage in a composite laminate is investigated. First of all, Figures 10, 11 and 12 give an indication on the effect that damage location and intensity have on the displacement. In fact, the value and the location of maximum displacement can sensibly vary when damaging one region rather than another one. An interesting example is represented by cases (a) and (c) in Fig. 10. In the first case, the location of the maximum displacement u_y is measured at the edge of the plate, $x = l/2$. On the other hand, when the damaged region is located near the application of the load (case (c)), there is a difference in terms of both value and location of the maximum displacement u_y, which is detected at $x > -l/2$. These differences are eliminated when a region covering the entire length of the plate is damaged, as in Fig. 11. As a matter of fact, cases (a) and (c) present here a perfectly symmetric behaviour, both in terms of location and intensity of longitudinal displacement. Numerical proofs of these consideration are reported in Table 3. Moreover, in this table, the coordinates of the point along the red line where u_y is independent from the damage intensity are also enlisted. The results presented in Fig. 12 show that damage has more influence on

		Case 8a	Case 8b	Case 8c	Case 9a	Case 9b	Case 9c
u_y max	Value [mm]	3.85	3.47	3.8	5.64	4.98	5.64
	Coordinate [mm]	25.0	0	-20.0	22.5	0	-22.5
Point A	Coordinate[mm]	-11.0	-	12.0	-11.0	-	11.0

Table 3: Value and location of the longitudinal displacement u_y in some representative points. Point A represents the point where the value u_y is independent from the damage intensity d.

the axial displacement when it is introduced in layers with 0 degrees orientation. On the other hand, a little influence is witnessed when the 90 degree-oriented layers are damaged. This outcome could have been easily predicted for the present case. However, different load conditions such as bending and shear will lead to a more complex response of the structure to a layer-wise damage. In these cases, high-order theories are required to accurately describe these phenomena. Figure 13 shows the variation in longitudinal displacement when various stacking sequences are adopted. As expected, different lay-ups lead to different structural responses, due to the change in the laminate properties. Thus, a CNN trained with a specific stacking sequence will not be able to provide accurate results for the testing of unseen laminates with different lay-ups.

5.1.4 Mesh convergence analysis

A final study before discussing damage detection problems is the convergence analysis shown in Fig. 14, which shows the influence of the mesh on the longitudinal displacement u_y. For this analysis, damage was introduced in the three central elements (case (b) in Fig. 11) and assigned to all the four layers. Both numbers of B4 element for the FEM discretization and LE9 elements for the thickness discretization have been increased. The convergence study for

three damage cases ($d = 0$, $d = 0.1$ and $d = 0.3$) has been reported in Fig. 14. It is clear that the first mesh with nine LE9 elements already provided accurate results in this particular structre.
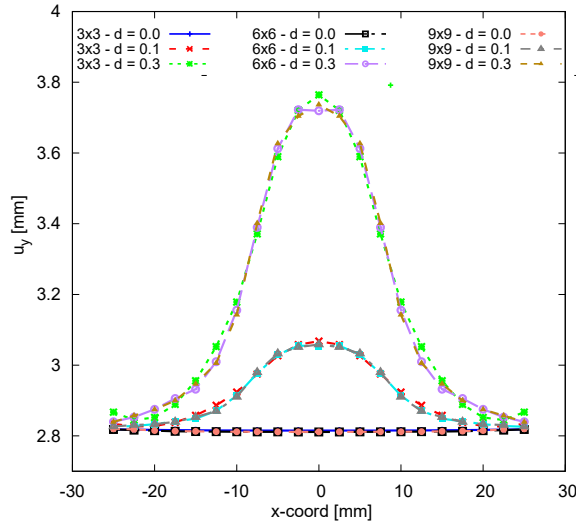

Figure 14: Effect of mesh discretization on longitudinal displacement u_y.

This last assessment could suggest that any finer mesh can be used to model any training and testing structure, without any loss in damage prediction accuracy. Nevertheless, in this case, displacements have been compared at one single fixed location. No information have been found about the behaviour of displacement in other regions of the plate. Thus, further analysis should be carried out to assure that a different mesh refinement will lead to the same complete displacement field.

5.2 Damage detection

The analysis from Section 5.1 show that damage obviously affect the way of deformation of structural components and that appropriate simulations and models are needed to detect this. The objective is now the training of a CNN in order to make it learn the damage-displacement/strain relationship for the solution of the inverse problem. In the following sections, both isotropic and orthotropic damage formulation will be adopted for the study of a composite laminate.

The field images adopted for training have a dimension of 413x413 pixels. The CNN architecture includes seven stacks of convolutional and average pooling layers. Filters with size 3x3 are applied in each convolutional layer, starting from a number of 8 filters for the first layer to a total of 512 for the last one. On the other hand, a 2x2 filter is applied to average pooling layers. Afterwards, two fully connected hidden layers are adopted. A learning rate of 0.001 is initially set, which is reduced by a factor 10 in the last ten epochs of the process. The stochastic gradient descent algorithm is adopted for CNN training. The aforementioned parameters have been the results of a trial-and-error procedure combined with some rules of thumb that have been developed in recent years across the scientific community [37]. The architecture proposed in this research is shown in Fig. 15.
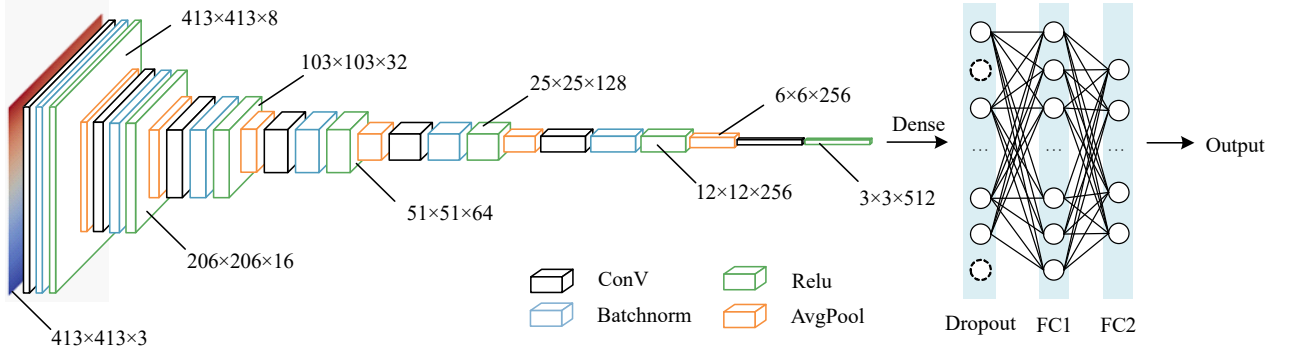
15

Figure 15: CNN architecture employed in the present work.

5.2.1 Isotropic damage

The same composite laminate proposed in previous sections is here analyzed for damage detection purposes. The isotropic damage formulation is here adopted to introduce damage in each region of the structure. In this case, a total of nine areas is identified, which means that the CNN should be able to predict nine damage parameters d, see Fig. 16. For training, these parameters are assigned through dedicated Monte Carlo simulations, with both mean and deviation standard equal to 0.1. It should be underlined that same damage is assigned to each layer of the single region. The boundary conditions consist of a uniaxial pressure applied on one edge, while the opposite edge is in a clamped condition.
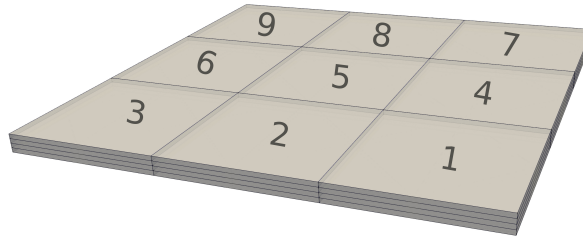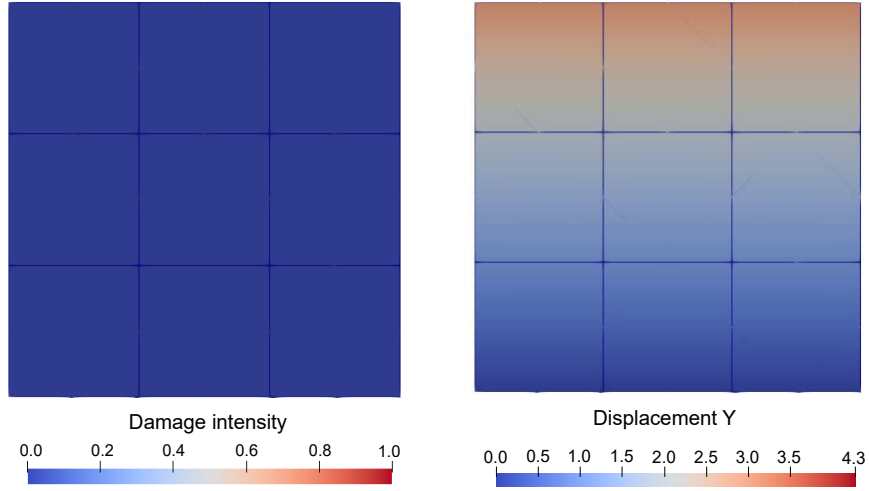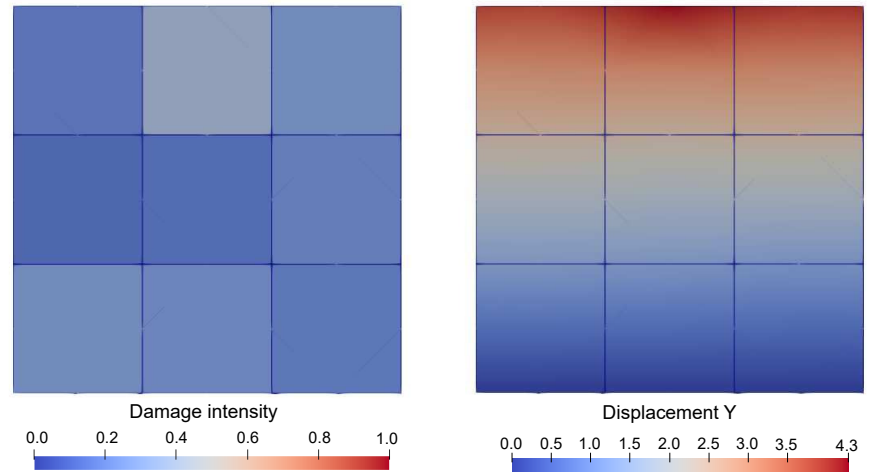

Figure 16: Numbering of the regions for the investigated plate.

An example of images for two different damage scenarios, pristine and randomly damaged structure, respectively, are represented in Fig. 17. In particular, axial displacements full-field maps measured on top surface of the laminate are used in this study. The CNN will be feed with a large number of these images from structures with a known damage distribution, with the final goal of being able to detect damage in unseen structures. Nevertheless, the appropriate number of images required to obtain an accurate prediction of damage intensity and severity should be object of a trade study. The aim is determining the lowest number of database samples which is needed to obtain the highest prediction accuracy possible. The proportion between numbers of sample employed as training, validation and test sets has been kept constant for all cases (i.e. 75%, 20 % and 5%, respectively). An NVIDIA GeForce GTX 1650 GPU has been employed for the CNN training process.

The index that has been considered for this convergence study is the regression coefficient R. This parameter gives information on how good is the neural network in predicting the targets. A value of $R = 1$ for a regression coefficient indicates that all target values are correctly predicted. The outcome of the convergence study is shown in Table 4. It is clear that a total number of 4000 samples already guarantees a good prediction accuracy by the

Damage intensity

0.0   0.2   0.4   0.6   0.8   1.0

Displacement Y

0.0 0.5 1.0 1.5 2.0 2.5 3.0 3.5   4.3

(a) Pristine structure

Damage intensity

0.0   0.2   0.4   0.6   0.8   1.0

Displacement Y

0.0 0.5 1.0 1.5 2.0 2.5 3.0 3.5   4.3

(b) Damaged structure

Figure 17: Longitudinal displacement fields of a pristine and damaged structure for the case of isotropic damage model.

Number samples	Time elapsed	Regression coefficient
4000	17min 47sec	0.9785
6000	27min 08sec	0.9837
8000	36min 23sec	0.9865
10000	48min 18sec	0.9902

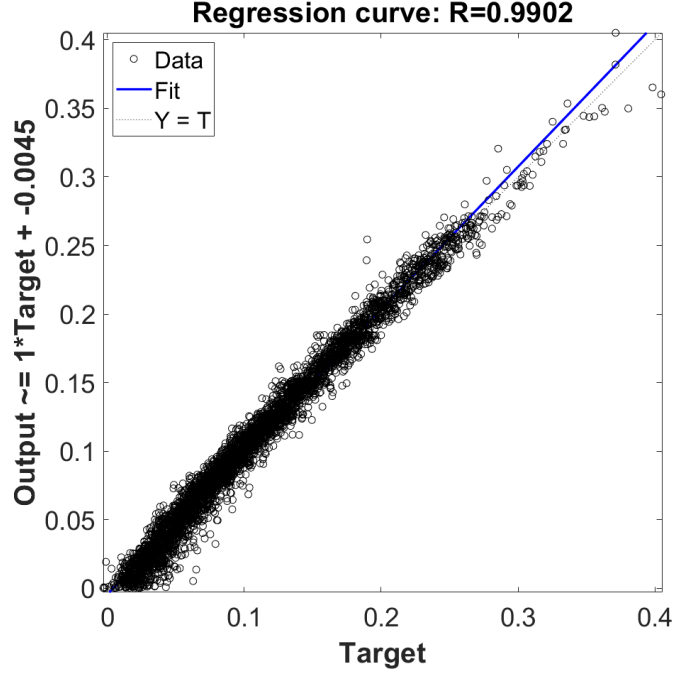Table 4: Convergence study for the case with isotropic damage model.

Figure 18: Regression curve for the case with isotropic damage model.

CNN, being the regression coefficient equal to 0.9785. A larger number of adopted samples leads to a better prediction accuracy, but the computational time for the CNN training will increase accordingly. Thus, a trade-off point between accuracy and computational time should be chosen, according to the required application.

Thereafter, some results are presented for the case with 10000 database samples. A total of 500 unknown structures have been fed into the trained neural network to verify if it is able to retrieve location and intensity of each damage in the structure. The regression curve is shown in Fig. 18. The regression coefficient R has a value near the unity, demonstrating an high accuracy in predicting the correct value of the CNN targets (i.e. damage). Figure 19 shows a comparison between the target value of damage intensity (red bars) and the CNN prediction in each region of the structure (blue bars) for two test samples, which are unknown for the CNN. In the vertical axis, the intensity of the damage is represented. In the horizontal axis, the numbering of the regions is displayed, following the repartition reported in Fig. 16.

5.2.2 Orthotropic damage

The previous case study, with same boundary and load conditions is here reproduced for the detection of orthotropic damages. The reduction factors d_1 (longitudinal damage) and d_2 (transversal damage) are introduced in each one of the nine regions through Monte Carlo simulations. Each layer of the same region will see the same damage intensities. Thus, the objective is now to predict the value of nine longitudinal damage d_1 and nine transversal damage d_2.

The first choice to be made is the field images to adopt for the network training. As first attempt, images of the longitudinal displacement fields have been employed as training images. The network's architecture has been maintained as in the isotropic damage case, with the only difference that the output layer will now have 18 neurons instead of nine. The outcome for both longitudinal and transversal damages is shown in Fig. 20. It is clear that the CNN is able

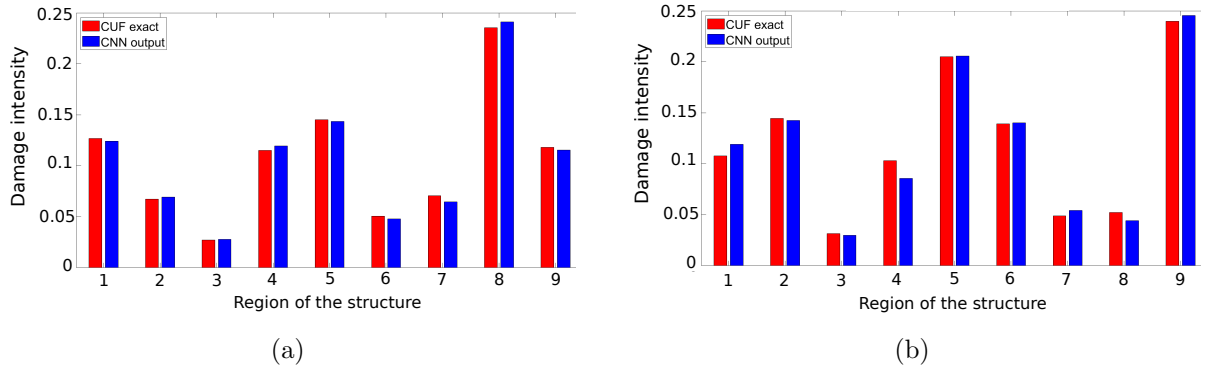(a)   (b)

Figure 19: Comparison between target value and CNN prediction in structures with all regions damaged for the case with isotropic damage model.
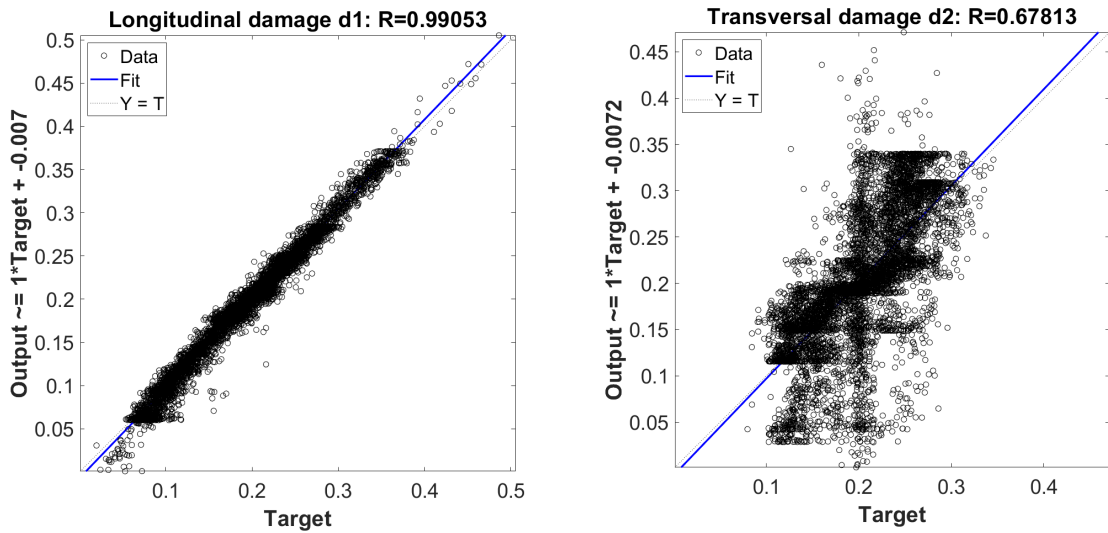

Figure 20: Regression curves for the case with orthotropic damage model by adopting longitudinal displacement images.
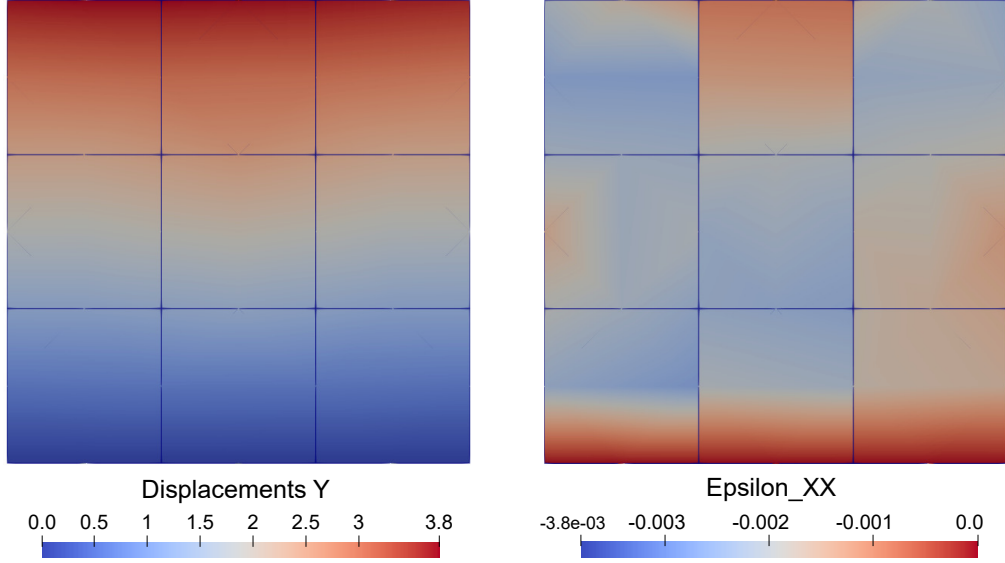
Figure 21: Example of axial displacement and normal strain field images for a randomly damaged structure for the case of orthotropic damage model.

to detect with significant accuracy the longitudinal damage d_1 in all nine regions involved, while the network has evident difficulties in predicting the transversal damage d_2. This situation could have easily been foreseen in advance. In fact, by employing only images of the axial displacement fields, the only information the CNN can retrieve are strictly related to the longitudinal damage d_1, while limited (or none) information are given about the transversal damage d_2 influence on the structure's behaviour. Thus, this choice of training images can not be considered adequate for the present case. A different approach is then used in order to solve the problem with orthotropic damage formulation. In fact, for each training sample a set of two images will be introduced as input: the longitudinal displacement field u_y and the normal strain field ε_{xx}. An example of training images from a randomly damaged sample is shown in Fig. 21. The objective is to give to the CNN sufficient information in order to accurately predict both d_1 and d_2 parameters.

Once the network training is performed with both displacement and strain data, the test images from unseen structures are introduced into the CNN for damage prediction. Results are shown in Fig. 22. One can notice that the CNN is still able to predict with good accuracy the longitudinal damage d_1, while a significant improvement is witnessed for the prediction of the transversal damage d_2. Nevertheless, it is also clear that the CNN performance in predicting d_2 is not as good as for d_1 parameter, showing a regression coefficient of 0.927 against the value of 0.984 for the longitudinal parameter. A trade study has then been performed to highlight the effect of the number of training samples. The outcome is shown in Table 5. It is evident from this results that there is an improvement in terms of accuracy when the number of samples increases. For this reason, it is safe to say that a larger database could lead to better predictions even for the transversal damage parameters.

As a final result and consistently to the case of isotropic formulation, a comparison between the network output (blue bars) and the target to be predicted (red bars) is shown in Fig. 23. The left graph refers to the longitudinal damages for each of the nine regions, while the right one refers to the transversal damage parameters.
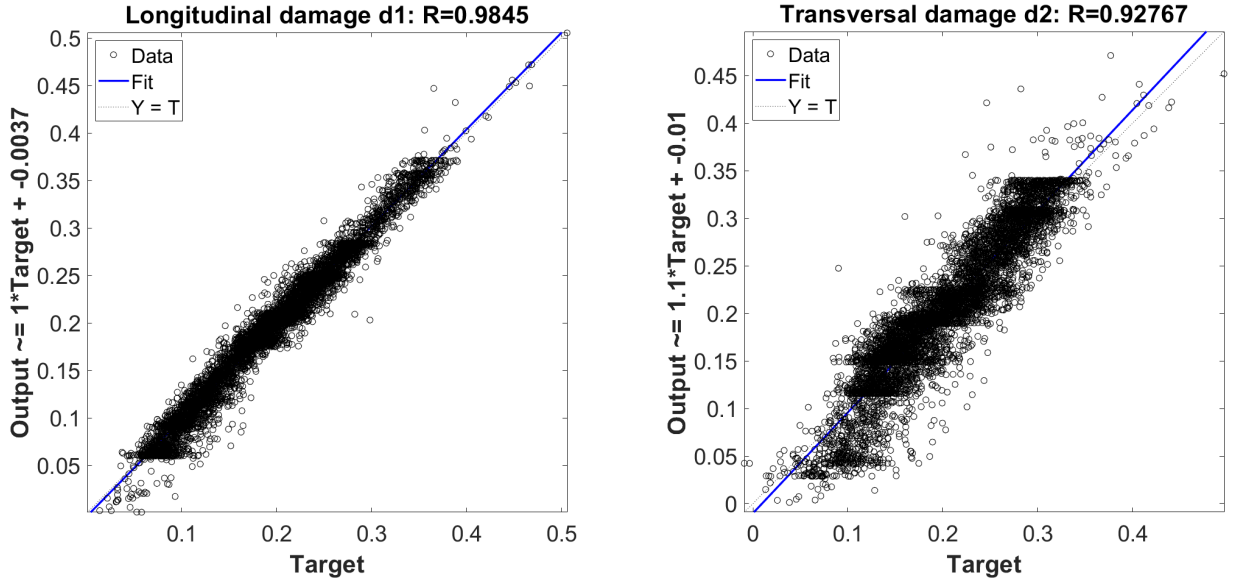
Figure 22: Regression curve for the case with orthotropic damage model by adopting both longitudinal displacement and normal strain images.

N samples	Time elapsed	Regression coeff. d_1	Regression coeff. d_2
8000	48min11sec	0.9577	0.8809
10000	58min55sec	0.9731	0.8848
12000	73min27sec	0.9798	0.9165
14000	96min24sec	0.9845	0.9276

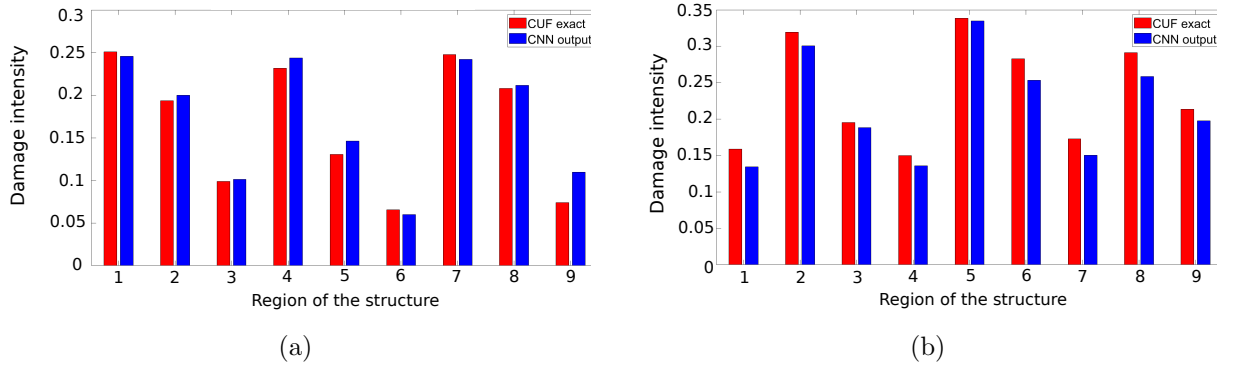Table 5: Convergence study for the case with orthotropic damage model.

Figure 23: Comparison between target value and CNN prediction in a structure with all regions damaged for the case with orthotropic damage model.

6   Conclusions

In this work, an Artificial intelligence (AI) technique has been coupled with high-order theory of structures by using the Carrera Unified Formulation (CUF). CUF capabilities are exploited in this paper to create an extensive simulation-based database for training of a Convolutional Neural Network (CNN). A fundamental CUF feature adopted in this work is the Component-Wise (CW) formulation, which allows the introduction of damages with different intensities for each component of the structure and leads to a better description of local phenomena. Damage was modelled as reduction of stiffness for each component in the structure. Two damage formulations have been implemented in the case of orthotropic composite structures. The isotropic formulation leads to a stiffness degradation of the same quantity d along the three directions, whereas, according to the orthotropic formulation, each component will see a damage d_1 for the longitudinal direction and a damage d_2 for the transversal one. A CNN is trained by choosing displacements or strains acquisitions or any combination of thereof. The trained network gives as output the location and intensity of each damage in a structure whose health status is unknown. This approach has been tested on a composite plate, considering both damage formulations. The results lead to the following considerations:

- CNN can predict with great accuracy both location and severity of damages in a multi-component structure. The simulation-based database adopted for CNN training and testing has been generated with no significant difficulty, due to the adoption of refined finite element, which guarantee 3D-like solution accuracy with a reduced computational cost.

- CW formulation allows a component-oriented damage localization in a multi-component structure. As a matter of principle, it is possible to consider distinct subportions of the entire domain, leading to a more precise localization. However, this could generate a more complex inverse problem to be solved.

- The use of strain/displacement field images to train a CNN appears to be a suitable approach to adopt when dealing with composite laminates. In fact, some difficulties have been encountered when a vibration-based damage detection method has been applied on composite plates in [31].

The promising results suggest future testing of the proposed approach through experimental measures, employing the Digital Image Correlation (DIC) technique for the evaluation of displacement and strain fields.

Acknowledgments

References

[1] K. Diamanti and C. Soutis. Structural health monitoring techniques for aircraft composite structures. *Progress in Aerospace Sciences*, 46(8):342–352, 2010.

[2] A Rytter. Vibration based inspection of civil engineering structures [P.h.D. thesis]. *Aalborg University*, 1993.

[3] S. Kessler and S. Spearing. Damage detection in composite materials using lamb wave methods. *Smart Materials and Structures*, 11:269, 04 2002.

[4] R.S.C. Monkhouse, P. Wilcox, M.J.S. Lowe, R.P. Dalton, and P. Cawley. The rapid monitoring of structures using interdigital lamb. *Smart Materials and Structures*, 9:304, 06 2000.

[5] X. Bao and L. Chen. Recent progress in distributed fiber optic sensors. *Sensors (Basel, Switzerland)*, 12:8601–39, 2012.

[6] R. Sante. Fibre optic sensors for structural health monitoring of aircraft composite structures: Recent advances and applications. *Sensors (Basel, Switzerland)*, 15:18666–713, 08 2015.

[7] S.Z. Zhang, Y.J. Yan, and Z. Wu. Electric potential detection for structural surface crack using coating sensors. *Sensors and Actuators A: Physical*, 137:223–229, 2007.

[8] M. Şahin and R. Shenoi. Vibration-based damage identification in beam-like composite laminates by using artificial neural networks. *Journal of Mechanical Engineering Science*, 217:661–676, 2003.

[9] A. Pagani, M. Enea, and E. Carrera. Component-wise damage detection by neural networks and refined fes training. *Journal of Sound and Vibration*, 509:116–255, 2021. ISSN 0022-460X.

[10] L. Grassia, M. Iannone, A. Califano, and A. D'Amore. Strain based method for monitoring the health state of composite structures. *Composites Part B: Engineering*, 176: 107253, 2019.

[11] H. Hwang and K. Cheol. Damage detection in structures using a few frequency response measurements. *Journal of Sound and Vibration*, 270:1–14, 02 2004.

[12] J. Zhou, Z. Li, and J. Chen. Damage identification method based on continuous wavelet transform and mode shapes for composite laminates with cutouts. *Composite Structures*, 191:12–23, 2018.

[13] Y. LeCun, L. Bottou, Y. Bengio, and P. Haffner. Gradient-based learning applied to document recognition. *Proceedings of the IEEE*, 86(11):2278–2324, 1998.

[14] M. Saadatmorad, R.A. Jafari-Talookolaei, M. Pashaei, and S. Khatir. Damage detection on rectangular laminated composite plates using wavelet based convolutional neural network technique. *Composite Structures*, 278:114656, 2021.

[15] J. Wu, X. Xu, C. Liu, C. Deng, and X. Shao. Lamb wave-based damage detection of composite structures using deep convolutional neural network and continuous wavelet transform. *Composite Structures*, 276:114590, 2021.

[16] S. Teng, G. Chen, G. Liu, J. Lv, and F. Cui. Modal strain energy-based structural damage detection using convolutional neural networks. *Applied Sciences*, 9:3376, 2019.

[17] M. Slonski and M. Tekieli. 2D digital image correlation and region-based convolutional neural network in monitoring and evaluation of surface cracks in concrete structural elements. *Materials*, 13:3527, 08 2020.

[18] N. Gulgec, M. Takáč, and S. Pakzad. Convolutional neural network approach for robust structural damage detection and localization. *Journal of Computing in Civil Engineering*, 33, 2019.

[19] Y. Wang, Q. Luo, H. Xie, Q. Li, and G. Sun. Digital image correlation (dic) based damage detection for cfrp laminates by using machine learning based image semantic segmentation. *International Journal of Mechanical Sciences*, page 107529, 2022.

[20] Bing P. Reliability-guided digital image correlation for image deformation measurement. *Appl. Opt.*, 48(8):1535–1542, 2009.

[21] M. Li, D. Jia, Z. Wu, Qiu. S., and W He. Structural damage identification using strain mode differences by the ifem based on the convolutional neural network (CNN). *Mechanical Systems and Signal Processing*, 165:108–289, 2022.

[22] A. Cabboi, C. Gentile, and A. Saisi. From continuous vibration monitoring to fem-based damage assessment: Application on a stone-masonry tower. *Construction and Building Materials*, 156:252–265, 2017.

[23] E. Carrera, M. Cinefra, M. Petrolo, and E. Zappino. *Finite Element Analysis of Structures through Unified Formulation.* John Wiley & Sons, 2014. ISBN 978-1-119-94121-7.

[24] R. Azzara, E. Carrera, M Filippi, and A. Pagani. Time response stress analysis of solid and reinforced thin-walled structures by component-wise models. *International Journal of Structural Stability and Dynamics*, 20:2043010, 11 2020.

[25] R. Azzara, E. Carrera, and A. Pagani. Nonlinear and linearized vibration analysis of plates and shells subjected to compressive loading. *International Journal of Non-Linear Mechanics*, 141:103936, 2022. ISSN 0020-7462.

[26] A. Pagani, M. Enea, and E. Carrera. Quasi-static fracture analysis by coupled three-dimensional peridynamics and high order one-dimensional finite elements based on local elasticity. *International Journal for Numerical Methods in Engineering*, 123(4):1098–1113, 2022.

[27] M.H. Nagaraj, J. Reiner, R. Vaziri, E. Carrera, and M. Petrolo. Progressive damage analysis of composite structures using higher-order layer-wise elements. *Composites Part B: Engineering*, 190:107921, 2020. ISSN 1359-8368.

[28] A. Racionero, R. Azzara, A. Pagani, and E. Carrera. Accurate stress analysis of variable angle tow shells by high-order equivalent-single-layer and layer-wise finite element models. *Materials*, 14(21), 2021.

[29] E. Carrera, A. Pagani, and M. Petrolo. Component-Wise Method Applied to Vibration of Wing Structures. *Journal of Applied Mechanics*, 80(4), 2013.

[30] E. Carrera, A. Pagani, and M. Petrolo. Free vibrations of damaged aircraft structures by Component-Wise analysis. *AIAA Journal*, 54:1–16, 2016.

[31] M. Enea, A. Pagani, and E. Carrera. Damage detection in composites by ai and high-order modelling surface-strain-displacement analysis. In *European Workshop on Structural Health Monitoring*, pages 330–337. Springer, 2023.

[32] E. Carrera and M. Petrolo. Refined beam elements with only displacement variables and plate/shell capabilities. *Meccanica*, 47(3):537–556, 2012.

[33] K.J. Bathe. *Finite element procedure.* Prentice hall, 1996.

[34] E. Carrera, A. Pagani, and M. Petrolo. Classical, refined and component-wise theories for static analysis of reinforced-shell wing structures. *AIAA Journal*, 51(5):1255–1268, 2013. doi: 10.2514/1.J052331.

[35] M. Shahbazi. *An efficient virtual testing framework to simulate the progression of damage in notched composite laminates.* PhD thesis, University of British Columbia, 2017.

[36] Y. Bengio, Y. LeCun, and D. Henderson. Globally trained handwritten word recognizer using spatial representation, convolutional neural networks, and hidden markov models. In J. Cowan, G. Tesauro, and J. Alspector, editors, *Advances in Neural Information Processing Systems*, 1993.

[37] C. Modarres, N. Astorga, E. Droguett, and V. Meruane. Convolutional neural networks for automated damage recognition and damage type identification. *Structural Control and Health Monitoring*, 25, 2018.